Generation and Annealing Behaviour of MeV Proton and ^{252}Cf Irradiation Induced Deep Levels in Silicon Diodes

J. Vanhellemont, A. Kaniava*, E. Simoen, M.-A. Trauwaert and C. Claeys[1]
IMEC, Kapeldreef 75, B-3001 Leuven, Belgium
*Permanent address: Vilnius University, Sauletekio ave. 10, 2054 Vilnius, Lithuania

B. Johlander, R. Harboe-Sörensen and L. Adams
ESTEC, European Space Agency, Noordwijk, Netherlands

P. Clauws
University of Gent (UG), Krijgslaan 281 S1, B-9000 Gent, Belgium

Abstract

The generation and annihilation of deep levels in diodes fabricated on n- and p-type floating zone and Czochralski silicon substrates is discussed as a function of the substrate parameters and the irradiation and thermal annealing conditions. Both low fluence irradiations with MeV protons and with the fission products of a ^{252}Cf source are investigated. The presence of deep levels with densities in the range of $4x10^{11}$ to $2x10^{12}$ cm^{-3}, is correlated with increase of the diode leakage current.

I. INTRODUCTION

Substrate damage introduced by incident high energy particles is one of the important radiation related problems encountered by electronic components in space or nuclear environments [1]. Accelerators to generate high energy particle beams are expensive and ^{252}Cf irradiation sources are frequently used as an affordable alternative to study hardening of technologies for space applications. In previous reports [2,3] it was shown that proton and ^{252}Cf irradiations create similar electrically active defects in silicon. The main differences are the damage generation rate per unit of fluence and the relative distribution of the different traps.

In the present paper results are presented of a study of the degradation and recovery of diode characteristics by proton and ^{252}Cf irradiations. The influence of oxygen and dopant concentration on the trap generation is discussed.

II. EXPERIMENTAL

Square diodes with different areas are fabricated on p-type floating zone (FZ) and Czochralski (Cz) wafers with interstitial oxygen content (O_i) between 6.5 and $8.6x10^{17}$ cm^{-3} according to the new ASTM standard [4], and on n-type FZ wafers as listed in Tables I and II. A first set of wafers receives no thermal pre-treatment (no) and the second set is subjected to a full internal gettering (IG) treatment. The internal gettering heat treatment consists of a 6h oxygen outdiffussion step at 1100°C, followed by a 8h nucleation step at 750°C in a N_2 atmosphere and a high temperature oxygen precipitation step for 110 min at 975°C in a 5% oxygen atmosphere. The last step corresponds with the oxidation step of the diode process. The full diode process is described elsewhere [2].

To address the impact of the interstitial oxygen content on the irradiation damage, p-type Cz wafers are used as listed in Table II. The starting interstitial oxygen content ($[O_i]$) is $7.3x10^{17}$ (wafers T1 and T3) and $8.6x10^{17}$ cm^{-3} (wafers T26 and T28), respectively. For comparison a pp^+ epi-wafer (T31) with a 10 μm thick epitaxial silicon layer and a FZ substrate (W7), both oxygen lean, are also included in the experimental matrix.

The diodes are irradiated at room temperature with the fission products of a ^{252}Cf source, which are mainly heavy ions with energies in the 100 MeV range [2], or with 10 or 100 MeV protons. The particle fluences are listed in Table III. Due to the non-uniformity of the 100 MeV proton beam, the following fluences were obtained for P5: W5: $4.06x10^{11}$ cm^{-2}, W7: $3.65x10^{11}$ cm^{-2} and W17: $2.0x10^{11}$ cm^{-2}.

After irradiation the recovery of the radiation induced substrate damage is studied by performing isochronal anneals for 15 min, increasing the temperature from 373K to 673K in steps of 50K.

Fourier transform infra red spectroscopy (FTIR) measurements are performed to determine the interstitial oxygen content after the diode processing as listed in Tables I and II.

Current/voltage (I/V) and capacitance/voltage (C/V) characteristics of the diodes are measured and correlated with results from the cross-sectional TEM investigation. The current/voltage characteristics of the diodes are measured using a HP 4145 parameter analyser. The potential of the back-side substrate contact is varied, while the front-side diode contact is

[1] Part of this work was performed under ESTEC contract 8615/90/NL/PM(SC). M.-A. Trauwaert is indebted to the National Science Foundation (IWONL) for her fellowship. A. Kaniava is indebted to the E.C. for his research fellowship.

0-7803-1793-9/$4.00©1994IEEE

Table I
Substrate types used in the present study

Wafer	Pre-treatment	Doping density N_D ($x10^{14}$ cm^{-3})	O_i after process ($x10^{17}$ cm^{-3})	Type
W3	IG	5.8	4.7	p Cz
W4	no	5.8	4.9	p Cz
W5	IG	20	4.5	p Cz
W7	IG	2	-	p FZ
W17	no	0.82	-	n FZ

Table II
Experimental matrix of p-type wafers with different interstitial oxygen content.

Wafer	N_D ($x10^{14}$ cm^{-3})	Pre-treatment	O_i after process ($x10^{17}$ cm^{-3})	Bulk defect density ($x10^9$ cm^{-3})	Width of denuded zone (μm)	Irradiation
T1	10	no	7.30	2	-	Cf4
T3	10	IG	7.28	1	-	Cf4
T26	9	no	4.23	50	2	Cf5
T28	9	IG	4.32	10	10	Cf5
T31	9	no	-	$> 10^3$	-	Cf4
W7	2	IG	-	-	-	Cf1

Table III
Irradiation conditions

	Energy (MeV)	Fluence (cm^{-2})	Label
^{252}Cf source		$3.92x10^6$	Cf1
		$7.0x10^6$	Cf2
		$1.16x10^7$	Cf3
		$6.13x10^6$	Cf4
		$6.39x10^6$	Cf5
Protons	10	$5.27x10^{10}$	P1
	10	$7.9x10^{10}$	P2
	10	$1.59x10^{11}$	P3
	10	$4x10^{11}$	P4
	100	$2 - 4x10^{11}$	P5

kept grounded. The system leakage is less than 1 pA. The current is measured through the smaller front contact. Attention has also been given to an accurate determination of the doping density by means of capacitance/voltage (C/V) analyses, using a 100 kHz, 30 mV ac modulation signal.

Capacitance DLTS, based on the lock-in principle, is used to determine the position in the band gap and the density and depth profile of the deep levels present within the depletion region of the diodes.

On some irradiated samples photoluminescence spectra are recorded after removal of the diode structure, for a further identification of the irradiation induced defects.

III. OBSERVATIONS

A. Diode characteristics

Before irradiation

Before irradiation the average diode leakage current density at -6V is of the order of 1-2 nA cm^{-2} except for wafer T26 (high oxygen, without IG treatment) where it is ten times higher.

During the diode process, about 50% of the interstitial oxygen in the wafers with the highest initial interstitial oxygen content (T26, T28) and less than 10% in the wafers with the low oxygen content (T1,T3), precipitates. Although the difference in the initial oxygen content is not large (from $7.3x10^{17}$ to $8.6x10^{17}$ cm^{-3}) the amount of precipitated oxygen [ΔO_i] increases non-linearly with initial [O_i] for conventional "high-low-high" annealing in agreement with the so-called S-curve [5].

The TEM analyses indicate that in the bulk of the high oxygen wafers a large density of precipitates is present of the order of 10^{10} cm^{-3}, i.e. $5x10^{10}cm^{-3}$ for T26 and $10^{10}cm^{-3}$ for T28. In the samples without pre treatment (T26), a shallow defect lean zone (DLZ), defined as the area in which no defects are observed with cross-section high voltage transmission electron microscopy, of about 2 μm is observed. In the internal gettered samples (T28), the DLZ is of the order of 10 μm. This observation shows that in T28 the precipitates are never "seen" by the depleted area while in T26, already for a reverse bias of about 5 V, the depleted area extends into the precipitate-rich bulk.

In the I/V characteristics a strong increase of the leakage current is indeed observed when the edge of the depletion region reaches and extends into the part of the substrate with the high oxygen precipitate density (Fig.1). A more detailed discussion on the impact of silicon oxide precipitates on the diode characteristics will be published elsewhere [6].

After irradiation

After irradiation an increase of the leakage current is observed which varies linearly with the irradiation dose for n- and p-type substrates although the current increase per unit of fluence is substrate dependent. For the gettered Cz wafers the leakage current is significantly lower and the correlation with the irradiation dose is less clear. Measurement of the leakage current as function of the diode area shows that perimeter leak-

age can be neglected and that the leakage current increase is mainly due to irradiation induced bulk damage inside the depleted area of the diodes. More extensive information on the impact of proton and ^{252}Cf irradiation on the diode leakage current is published elsewhere [2,3,7].

After all irradiations the C/V measurements reveal that the diodes show the same active doping density as before, indicating that the density of traps is much smaller than the doping concentration.

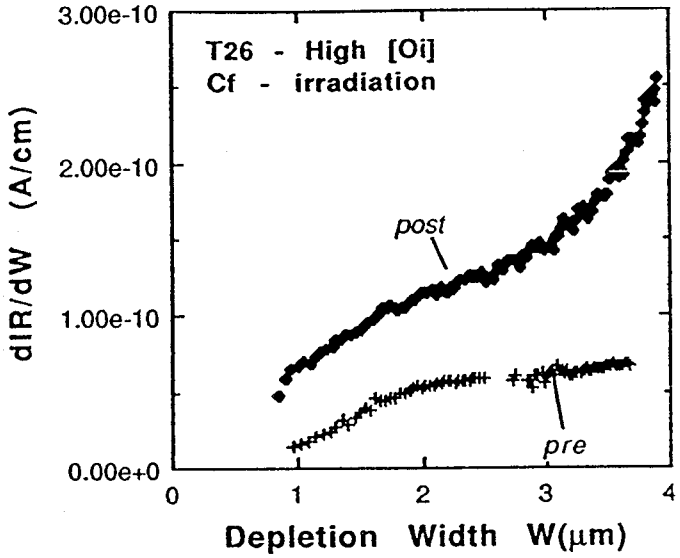

Fig. 1 Increase of reverse current before and after irradiation Cf5 as a function of depletion width. Taking into account the junction depth of 0.5 μm, the 2 μm denuded zone is clearly reflected in the profile before irradiation.

B. DLTS results

Before irradiation

The DLTS measurements correspond well with the leakage current results and confirm the good quality of the diodes. As for the leakage currents, diode T26 behaves however different. Increasing the depletion width in T26, leads to the observation of two minority traps (E_C - 0.17eV and E_C - 0.43eV). The second one, located closest to mid-gap can directly be correlated with the leakage current increase. Depth profiles of leakage current increase and deep level density, correspond very well with each other and with the TEM observations. A more detailed discussion of the correlation between silicon oxide precipitates and minority carrier traps observed with DLTS will be published elsewhere [8].

After irradiation

DLTS measurements reveal the formation of deep levels which are also observed after high energy electron or proton irradiation [2,3]. A typical DLTS spectrum is shown in Fig 2. In p-type silicon, the dominant deep levels are interpreted as related with the di-vacancy V_2 (H4, 0.21 eV) and with a carbon-oxygen C_iO_i or carbon-carbon C_iC_s related complex (H5, 0.36 eV). Interesting to notice is that the minority carrier traps E_C-0.43 eV, which are present in the sample T26 before irradiation and which are associated with the occurrence of silicon oxide precipitates inside the depleted area, are still present after irradiation as illustrated in Fig. 3.

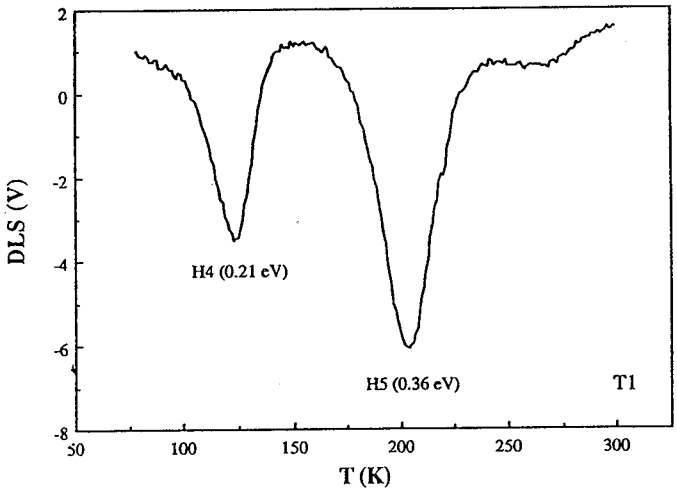

Fig. 2 Typical DLTS spectrum recorded on wafer T1 after ^{252}Cf irradiation.

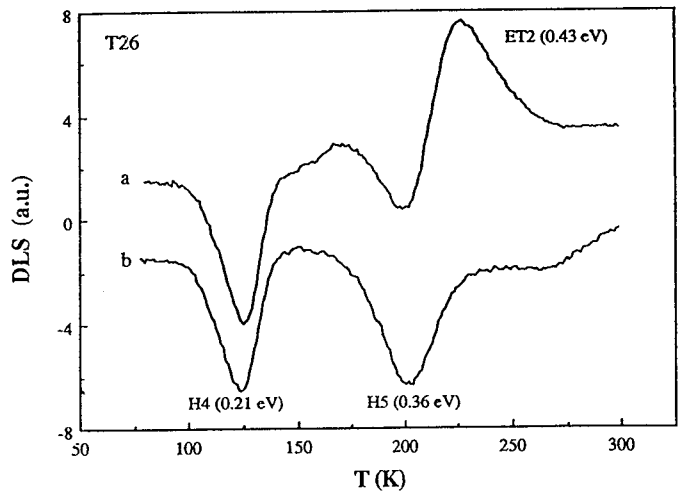

Fig. 3 DLTS spectra recorded on wafer T26 with (top) and without minority carrier injection.

In agreement with the leakage current measurements, DLTS reveals much smaller peak amplitudes for the Cz wafers. Most probably the large number of precipitates and the high concentration of interstitial oxygen deeper in the bulk form an effective sink for the vacancies and self-interstitials which are the primary defects created during the irradiation, thus leading to lower defect concentrations in the active depletion area of the diodes. Cz wafers with high oxygen content

are thus more radiation hard than FZ wafers with respect to deep level generation. The same deep levels are introduced both by proton and ^{252}Cf irradiations but the relative distribution and the generation rate of the traps is particle dependent. The number of deep levels generated per unit of fluence is about 10^5 times larger for ^{252}Cf irradiation than for proton irradiation similar to the increase of the leakage current per unit of fluence [3].

Table IV gives an overview of the different traps which are observed in the present study together with the associated lattice defect as reported in literature.

Table IV
Characteristics of ^{252}Cf irradiation induced deep levels. $\sigma(\infty)$ is the capture cross-section as determined from a conventional Arrhenius plot while $\sigma(T)$ is directly measured at the peak temperature, by varying the DLTS filling pulse length.

Wafer	Deep level	ΔE (eV)	$\sigma(\infty)$ ($\times 10^{-16}$ cm^2)	$\sigma(T)$ ($\times 10^{-16}$ cm^2)	Lattice defect
W17	E1	0.17	13	0.24-1.3 (90 K)	$VO^{-/0}$ A-center
	E2	0.23	5.5	0.31 (133 K)	$V_2^{--/-}$
	E3	0.42	23	1.1 (228 K)	$VP^{-/0}$ E-center + $V_2^{-/0}$
	HT1	0.35	13	-	$C_i O_i$
W7	H4	0.19	6.1	0.35-0.73 (123 K)	$V_2^{0/+}$
	H5	0.36	19	0.7-1.8 (203 K)	$C_i C_s^{0/+}$ and/or $C_i O_i^{0/+}$
	ET1	0.24	73	-	$B_i O_i$

The impact of the starting interstitial oxygen content on the deep level distribution is illustrated in Table V, listing observations after ^{252}Cf irradiation. As W7 has a lower doping density, one has to take into account that a larger fraction of the damage peak is probed with DLTS. Nevertheless it is clear that the concentration of level H4 does not depend on the oxygen content and status, while CH5 varies strongly with starting oxygen content.

Fig. 4 summarises the observed deep level density per unit of fluence both for the proton and ^{252}Cf irradiated p-type substrates, as a function of the boron concentration. The results for the wafers doped with 2, 5.8, 9 and 10×10^{14} B cm^{-3} can be compared as the depleted region is similar (of the order of 5 μm). For the 20×10^{14} B cm^{-3} doped wafer the depleted area is only of the order of 2.5 μm so that only the tail of the damage profile is addressed and the observed trap concentration thus too low. Nevertheless the results show that deep level generation is more efficient in FZ substrates and increases with boron concentration.

Table V
Summary of DLTS observations obtained with a reverse bias of -15V after irradiations Cf4, Cf5 and Cf1

Wafer	PT	Majority carrier traps ($\times 10^{11}$ cm^{-3})		Ratio	Minority carrier traps ($\times 10^{11}$ cm^{-3})	
		CH4 (0.19 eV)	CH5 (0.36 eV)	CH5/CH4	SiO_x related	Radiation induced
T1	no	5.4	9.4	1.75	-	-
T3	IG	6.4	9.7	1.5	-	-
T26	no	6.1	6.0	1.0	0.43 eV $\sigma_n = 10^{-14}$ cm^{-2} 7.5-10 T = 240K	-
T28	IG	6.1	4.3	0.7	-	-
T31	no	7.0	4.8	0.7	-	-
W7	IG	6.5	20	3.1	-	0.24 eV (B_i-O_i) 5.7

The densities of the irradiation-induced and SiO_x related deep levels derived from DLTS peak amplitude for majority and minority carriers are presented in Table V. For the fluence used in the present study the densities of the SiO_x-related and irradiation induced traps is similar. As expected, the resulting increase of leakage current is also of the same order of magnitude as the one due to the SiO_x centres (Fig. 1) and similar for all p-type substrates studied. Additional data obtained on p-type FZ material irradiated with a lower ^{252}Cf fluence, are included in the table for comparison.

Consideration must be given concerning the depth of the wafer which is probed by the DLTS method. The standard reverse bias applied to the samples is -15 V. The corresponding depletion width is about 5 μm for the samples with doping density $N_B = 9\times10^{14}$ cm^{-3}. Thus, only a part of the radiation damage profile is probed under these measurement conditions.

Beside the radiation damage profile, there is a non uniform distribution of interstitial oxygen due to outdifussion and precipitation of oxygen as was mentioned above. In spite of the complicated superposition of those two depth profiles, some general conclusions can be drawn regarding the dependence of radiation-induced defects on interstitial oxygen concentration. The density CH4 of di-vacancies (V_2) is independent of the interstitial oxygen content (integrated through the thickness of

wafer) as well as of the thermal pre treatment. For the wafers T1,..,T31 the density CH5 of the interstitial carbon- interstitial oxygen complexes (C_i-O_i), and the ratio of densities CH5/CH4 increases with the amount of interstitial oxygen which remains after the full diode process.

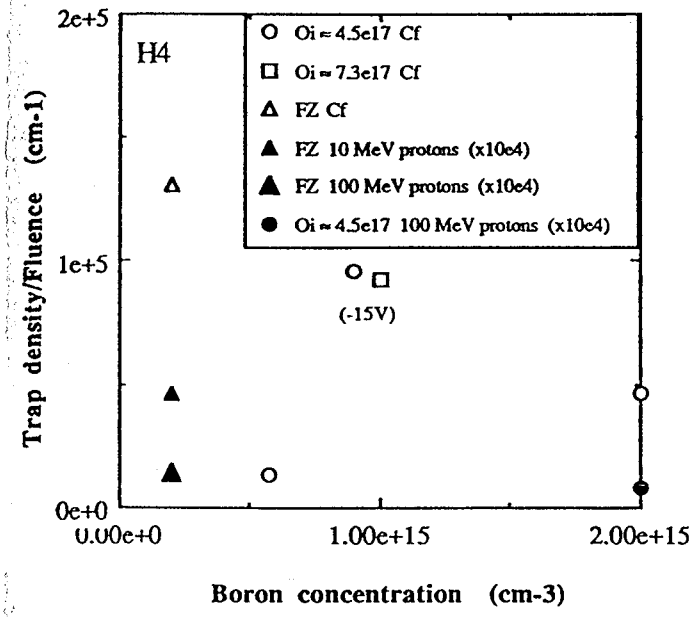

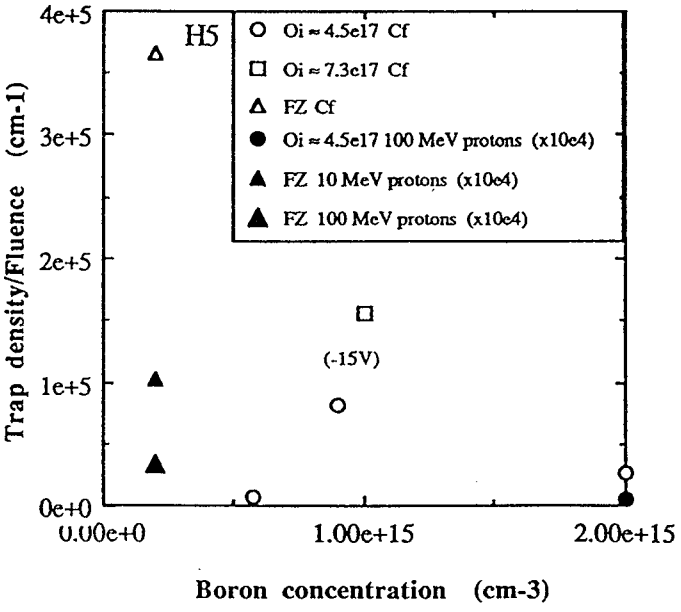

Fig. 4 Concentration per unit of fluence of the two dominant majority carrier traps in p-type silicon as a function of boron concentration and for different oxygen contents. The samples with boron concentrations of 9 and $10x10^{14}$ cm^{-3} have been measured with a reverse bias of 15V. The other samples were measured with a reverse bias of 6V.

Although the average density of $[O_i]$ in wafers T26 and T28 (also in T1 and T3) is the same (see Table II), due to different thermal processing, the radiation sensitivity of sample T28 (IG) with initial high value of $[O_i]$ is similar to the one of the oxygen-poor epi-wafer T31. Due to the small denuded zone in sample T26, the peak of the interstitial oxygen concentration lies within the depletion region which explains the higher value for CH5. In sample T28 this peak lies much deeper than the depletion width so that the part of the denuded zone which is addressed with DLTS compares very well with the oxygen-lean epi wafer T31.

The leakage current measurements show an opposite tendency: diodes T1 and T3 show a 20% lower leakage current than diodes T26 (after correction for the precipitate contribution), T28 and T31 although the density of H5, which is the dominant level contributing to the leakage current due to its position closest to the middle of the band gap, is 50% to 200% higher in T1 and T3. Two possible explanations are: either the presence of minority or majority traps which are not detected by DLTS or an influence of the high precipitate and defect density which is present deeper in the bulk in T26, T28 and T31.

Trap generation in FZ silicon

A somewhat surprising result is also obtained for the FZ wafer where CH5 is much larger than in the other wafers. Investigation with photoluminescence (PL) showed however that in wafer W7, the deep level H5 is connected only with the presence of interstitial carbon/substitutional carbon complexes (PL line 969.5 meV [9]) while in the Czochralski wafers only the C_iO_i complex (PL line 789.4 meV [9]) can be detected with PL. It is well documented that both types of defects introduce deep levels with the same position in the bandgap and can thus not be resolved in a straightforward way using DLTS. As wafer W7 has a ten times lower dopant concentration, the depletion width for a filling pulse between -10 and -0.5 V corresponds with the position of the maximum of radiation damage (≈ 9 μm) making it possible to measure accurately the depth profiles of the different traps by using the Double-DLTS (DDLTS) technique. The observations show that the peak concentration for the di-vacancy lies somewhat closer to the surface than that of the self-interstitial related defect C_iC_s, which might be due to the knock-on effect by which the self-interstitial after its creation is driven deeper towards the substrate while the vacancy is left behind [8].

The depletion width in the FZ sample under zero reverse bias is large enough (about 2 μm) to perform also a DLTS measurement of minority carrier emission by applying only an injection pulse, i.e. from 0 to 1.0 V. An electron trap with activation energy E_C-0.24 eV and an estimated concentration $N_t \approx 6x10^{11}$ cm^{-3} is observed (Fig. 5a). The origin of this level is well documented in the literature and can be related either with the di-vacancy in the negative charge state (0.23-0.25 eV) or with the interstitial boron-interstitial oxygen complex (B_i-O_i, 0.27 eV) [10,11].

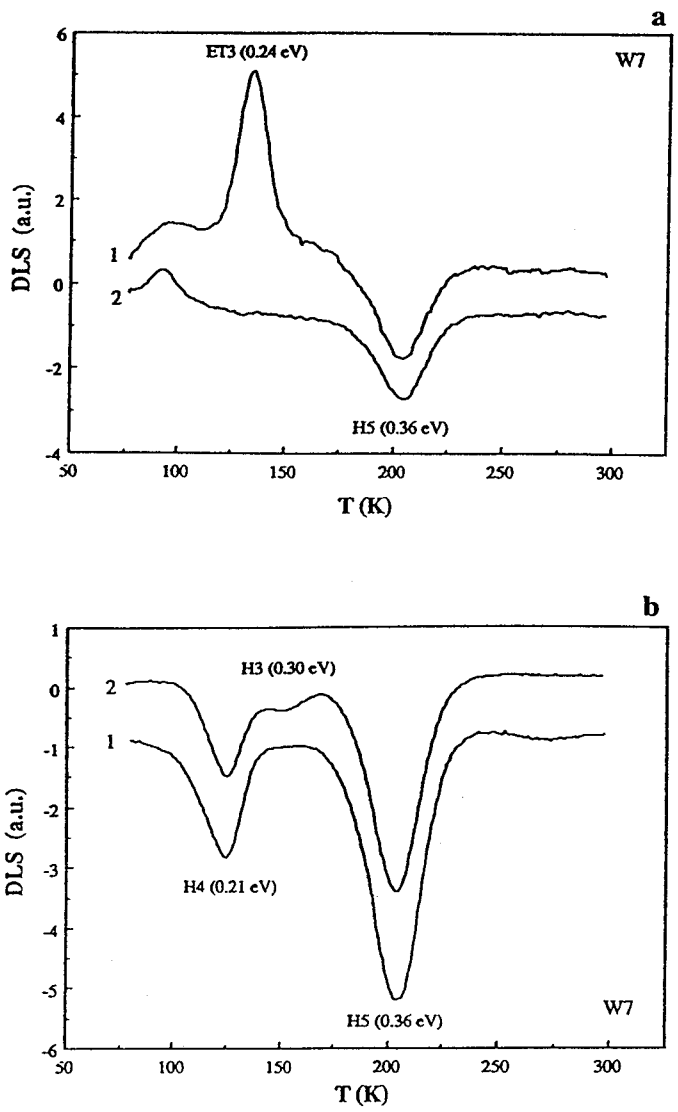

Fig. 5 a) DLTS spectra recorded on wafer W7 after irradiation Cf1, before (top) and after anneal at 523K for 15 min. The spectra are recorded with a filling pulse between 0 and 1 V thus revealing also the minority carrier capture levels.
b) DLTS spectra obtained on the same specimen using a filling pulse from -10 to 0.5 V. The top spectrum is the one after the thermal anneal and reveals a new majority trap at around 155 K, corresponding with a V-O-B complex.

To clarify this uncertainty, the FZ sample is annealed for 15 min at T = 523K in an argon atmosphere. The di-vacancy related defect is known to anneal out at 573K, whereas the B_i-O_i complex is stable below 473K [11,12]. As illustrated in Fig. 5b, after annealing, the disappearance of the electron trap E_c-0.24 eV is accompanied by the emergence of a new hole trap at E_v+0.30 eV while the amplitude of the hole trap E_v+0.21 eV decreases by about 25% showing only partial annealing of di-vacancies.

A similar sequence of annealing of the deep levels at temperatures in the range of 523-573K has been observed in electron and α-particle irradiated p-type silicon [13] and attributed to the transformation of the B_i-O_i complex to a vacancy-oxygen-boron (V-O-B) complex.

C. Annealing experiments

The irradiated FZ wafers were chosen for the annealing experiments as more sensitive DLTS measurements are possible due to the lower background doping.

In Fig. 6 the density of H4 and H5 traps in a p-type FZ diode are plotted versus the isochronal anneal temperature. The vacancy related deep level is stable up to 500K, while the carbon/oxygen related center anneals out around 640K.

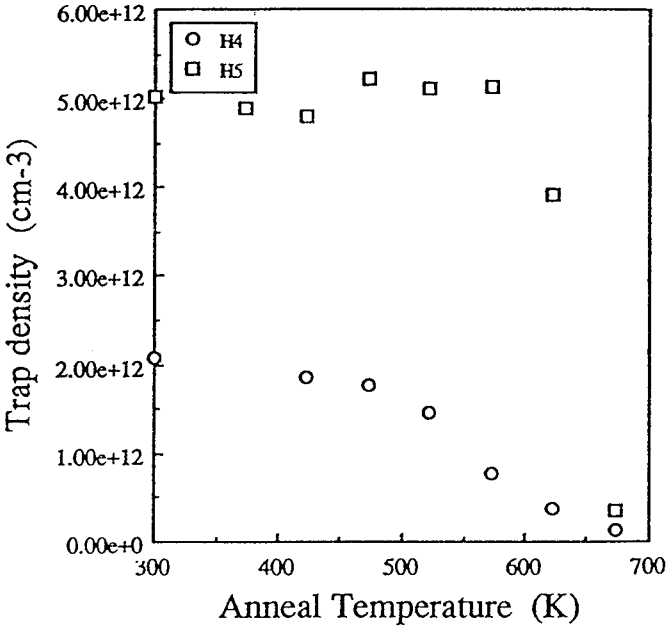

Fig. 6 Effect of 15 min isochronal anneals on the hole trap densities CH4 and CH5 in W7 after irradiation Cf3.

In Fig. 7 the same graph is given for the E1, E2 and E3 traps in the n-type FZ diode. A two step anneal is observed for the E3 level: a first one occurs at about 400K while a second occurs at around 570K.

In Fig. 8, three DLTS spectra are shown, recorded after three isochronal anneals, illustrating the initial increase of the A-center density at the expense of both di-vacancy related centers. In Figs. 9 and 10, the results of isothermal annealing of W17 (Cf2) at 573K and W7 (Cf2) at 623K are shown.

For the n-type substrates, the observed two anneal stages of the E3 level correspond well with the stability temperature values reported for the E-center (423K) and the di-vacancy (573K), respectively [14,15]. The initial fast increase of the concentration of the A-centre and the di-vacancy during the anneal at 573K, can be explained by the instability of the E-centre which will release rapidly vacancies which are partly captured by the interstitial oxygen and partly form di-vacancies.

For longer anneal times the annealing behaviour of the E2 and E3 level are similar, confirming that both levels can be different charge states of the same lattice defect, i.e. the di-vacancy.

From the isothermal annealing behaviour of the trap concentration CT, one can calculate the annihilation rate r using

$$CT(t) = CT(0)\, e^{-rt} \quad . \qquad (1)$$

The annihilation rate r(T) itself is temperature dependent and one can estimate its activation energy E_a from the isochronal annealing results. Assuming an isochronal annealing time t_a and an increase of anneal temperature T_i one can write

$$r(T) = r_0\, e^{-\frac{E_a}{kT}} \quad , \qquad (2)$$

and

$$\frac{CT(T + T_i)}{CT(T)} = e^{-r(T + T_i)t_a} \quad . \qquad (3)$$

The results of this calculation are listed for H4 and H5 in Table VI. Due to the limited number of data points, the E_a values obtained in the present work are only first order estimates. The value obtained for the di-vacancy is however the same as the one reported for the anneal of the di-vacancy (E2) in n-type material [14].

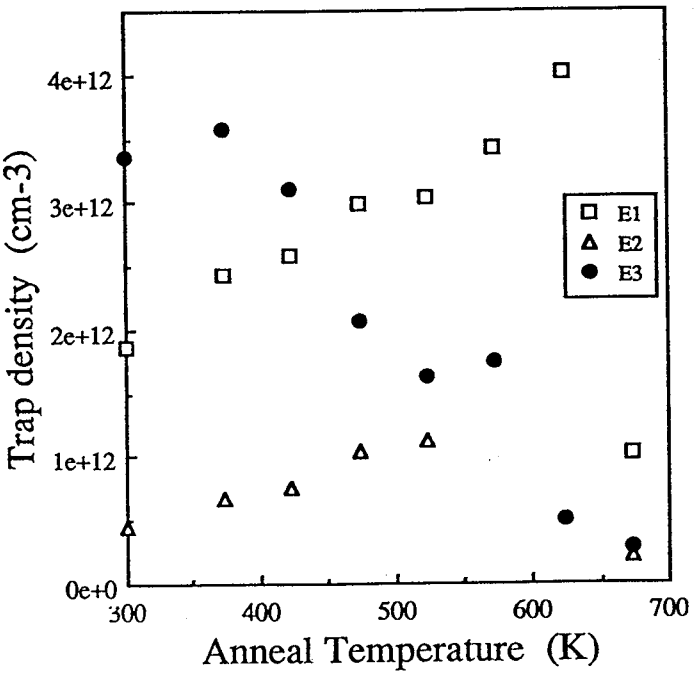

Fig. 7 Effect of isochronal anneals on the electron trap densities CE1, CE2 and CE3 in W17 after irradiation Cf3.

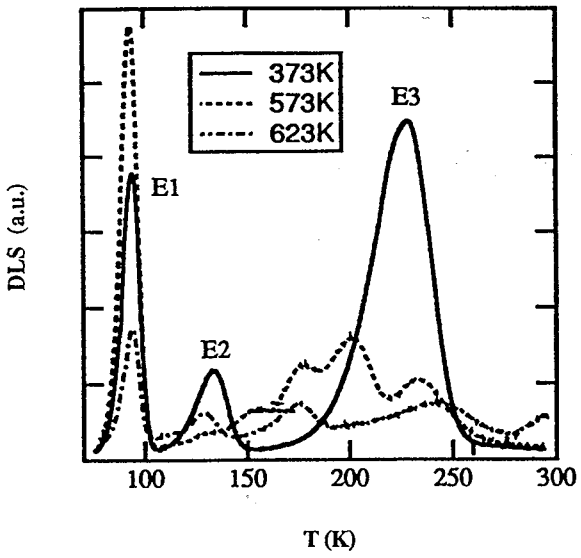

Fig. 8 DLTS spectra obtained after isochronal anneals at three different temperatures of W17 after irradiation Cf3.

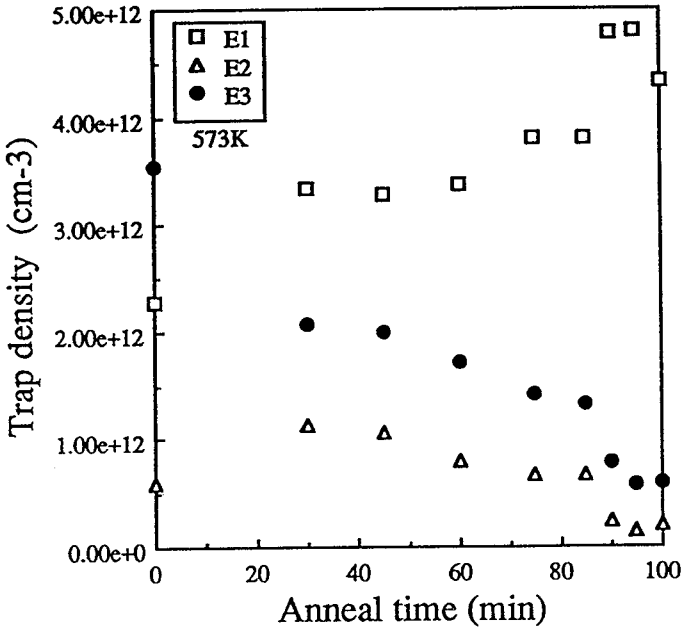

Fig. 9 Isothermal anneal at 573K of levels E1, E2 and E3 in W17 after irradiation Cf3.

Table VI

Trap annihilation rate r and its activation energy E_a for levels H4 and H5, calculated from the isothermal and isochronal anneals

Trap	Anneal temperature (K)	r ($x10^{-5}$ s^{-1})	E_a this work (eV)
H4 (V_2)	623	45	1.3
H5 (C_iC_s)	623	32	0.95

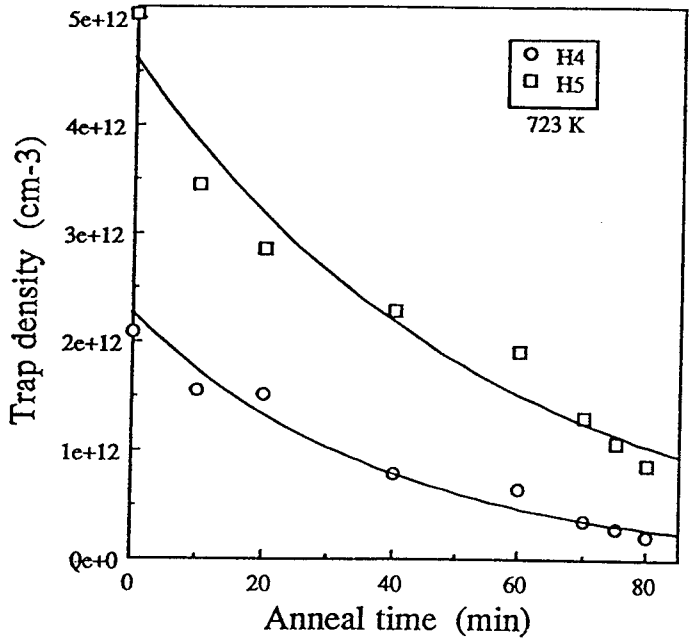

Fig. 10 Isothermal anneal at 623K of H4 and H5 in W7 after irradiation Cf3.

IV. CONCLUSIONS

SiO_x precipitates are responsible for strong minority carrier traps in p-type silicon. Two deep levels, i.e. E_C-0.17 eV and E_C-0.43 eV can be related with SiO_x precipitates. The observed minority traps are responsible for the increase of the leakage current of the diodes before irradiation.

The diode leakage current increase due to high energy particle irradiation, is mainly due to a combination of minority and majority carrier traps close to the middle of the bandgap, occurring with densities ranging from $4x10^{11}$ to $2x10^{12}$ cm^{-3}.

In irradiated p-type silicon substrates the dominant majority carrier traps contributing to the leakage current are interstitial related traps, i.e. the C_iC_s related trap in FZ silicon and the C_iO_i related trap in oxygen-rich Cz silicon. Both traps are located at about 0.35 eV above the valence band. The concentration of di-vacancy levels is independent of the oxygen content and thermal pre-treatments.

In irradiated n-type silicon substrates the dominant majority carrier traps contributing to the diode leakage current at room temperature are both vacancy related, i.e. the E-center (PV complex) and the di-vacancy.

The observed annealing behaviour of the dominant radiation induced traps in FZ silicon strengthens their preliminary identification which was based on the DLTS results. The conversion of the electron trap (E_C-0.24 eV) to a hole trap (E_V+0.30 eV) during annealing at temperature 523K can be interpreted as the transformation of the interstitial boron-interstitial oxygen complex into a vacancy-oxygen-boron complex in ^{252}Cf irradiated p-type FZ silicon.

An important unresolved problem is the in some samples observed lack of correlation between the leakage current increase after irradiation and the deep level increase.

V. REFERENCES

[1] C. Claeys, E. Simoen and J. Vanhellemont, "Proton Irradiation of Silicon. Literature review", report P35271-IM-RP-0005, ESTEC contract 8615/90/NL/PM(SC)-COO8-WO7, 1991.

[2] C. Claeys, E. Simoen, M.-A. Trauwaert and J. Vanhellemont, "Electrical and Physical Characterization of Proton and Cf-252 Bulk Radiation Damage", report P35271-IM-RP-0017, ESTEC contract 8615/90/NL/PM(SC)-COO8-WO7, 1992.

[3] M.-A. Trauwaert, J. Vanhellemont, E. Simoen, C. Claeys, B. Johlander, L. Adams and P. Clauws, "Study of Electrically Active Lattice Defects in Cf-252 and Proton Irradiated Silicon Diodes", *IEEE Trans. Nucl. Science* , NS-39(6), pp. 1747-1753, December 1992.

[4] Annual Book of ASTM standards, ASTM Philadelphia 1985 (p.242).

[5] H-D Chiou, "Criteria for choosing initial oxygen concentration in Cz silicon wafers", *The Electrochemical Society Proceedings Volume* , 91-9, pp. 577-588, 1991.

[6] E. Simoen, J. Vanhellemont, A. Kaniava and C. Claeys, "Impact of oxygen-related defects on the electrical characteristics and the degradation of Si n^+p junctions", accepted for presentation at symposium "*The degradation of electronic devices due to device operation as well as crystalline and process-induced defects*" of The Electrochemical Society Fall Meeting, New Orleans, October 10-15 (1993), to be published in *The Electrochem. Soc. Proc. Vol.*

[7] J. Vanhellemont, E. Simoen, A. Kaniava, M.-A. Trauwaert, C. Claeys, B. Johlander, R. Harboe-Sörensen, L. Adams and P. Clauws, "Electrical impact of proton and ^{252}Cf irradiation induced traps in silicon diodes", in proceedings of 2nd ESA Electronic Components Conference (EECC'93), Noordwijk (Netherlands), in press, 1993.

[8] A. Kaniava, J. Vanhellemont, E. Simoen and C. Claeys, "Deep Levels in Heat Treated and ^{252}Cf Irradiated p-Type Silicon Substrates with Different Oxygen Content", submitted for publication in *Radiation Effects and Defects in Solids.*

[9] O.O. Awadelkarim, H. Weman, B.G. Svensson and J.L. Lindström, "Deep-level transient spectroscopy and photoluminescence studies of electron-irradiated Czochralski silicon", *J. Appl. Phys.*, 60(6), pp. 1974-1979, 1986.

[10] H.J. Möller, Semiconductors for Solar Cells, (Artech House, Norwood, 1993), ch5 pp. 107-153.

[11] P.J. Drevinski, C.E. Caefer, S.P. Tobin, J.C. Mikkelsen,jr and L.C. Kimerling, "Influence of oxygen and boron on defect production in irradiated silicon", *Mat. Res. Soc. Symp. Proc.*, vol. 104, pp. 167-172, 1988.

[12] P.J. Drevinsky, C.E. Caefer, L.C. Kimerling and J.L. Benton, "Carbon-related defects in silicon", in "*Defect Control in Semiconductors*", ed. K. Sumino, Elsevier Science Publishers B.V. (North-Holland), pp. 341-345, 1990.

[13] M. Asghar, M. Zafar Iqbal and N. Zafar, "Study of alpha-radiation-induced deep levels in p-type silicon", *J. Appl. Phys.*, 73 (9), pp.4240- 4247, 1993.

[14] S.D. Brotherton and P. Bradley, "Defect production and lifetime control in electron and γ-irradiated silicon", *J. Appl. Phys.*, 53 (8), pp. 5720-5732, 1982.

[15] M. Asghar, M. Zafar Iqbal and N. Zafar, "Characterization of deep levels introduced by alpha radiation in n-type silicon", *J. Appl. Phys.*, 73 (8), pp.3698-3708, 1993.